Hindawi
Advances in Materials Science and Engineering
Volume 2023, Article ID 9321342, 8 pages
https://doi.org/10.1155/2023/9321342

Research Article

Steel Pipe Internal Corrosion Protection Using Magnesium Anode: Impact of Protective Potential and Phase Layer Formation on Corrosion Rate

Georgii Vasyliev and Yuriy Gerasymenko

National Technical University of Ukraine "Igor Sikorsky Kyiv Polytechnic Institute", 37, Prospect Peremohy, Kyiv 03056, Ukraine

Correspondence should be addressed to Georgii Vasyliev; g.vasyliev@kpi.ua

Received 23 October 2022; Revised 20 November 2022; Accepted 25 January 2023; Published 2 February 2023

Academic Editor: Hany Abdo

The influence of magnesium anode dissolution in pipe filled with potable water on the steel corrosion rate was investigated. Steel corrosion rate was measured using the weight loss technique, and linear polarization resistance measurements were used to estimate the formation kinetics and protective abilities of the phase layer on the metal surface. The cathodic current distribution along steel pipe was measured using a microammeter and compared with the computer model. The results clearly demonstrate that the reduction of metal corrosion rate is at least 2.8 times in the region where cathodic protection distributes inside the pipe. However, for the remaining part of the metal pipe, the reduction of corrosion rate of 1.5 times was obtained due to the formation of the phase layer on the metal surface that leads to the reduction of oxygen supply. The results obtained in the study can be further applied for designing and maintenance of water supply systems.

1. Introduction

Corrosion of metal equipment is an inevitable process in all branches of industry that causes billions of direct losses annually; moreover, indirect losses are even more expensive. Corrosion problems in water pipeline systems not only lead to metal losses but also cause failures, unstable water supply, and water quality deterioration. Steel remains the most widespread construction material for new pipelines and many more pipelines that were constructed in the last 50 years. Due to sanitary restrictions on the application of chemical reagents, internal corrosion reduction of steel water supply pipelines remains a challenging task both from technological and economical points of view.

Generally accepted approach to corrosion protection in water supply systems is based on the ability of natural water to form a phase layer on the surface of the corroding metals that slows down or even prevents further corrosion [1]. Several indices were proposed to evaluate water corrosion aggressivity based on water composition: Langelier saturation index, Ryznar index, etc. [2, 3]. Phase layer consists of steel corrosion products, namely, oxides and oxyhydroxides of iron, and calcium carbonate [4–7]. The composition and structure of the phase layer will determine its protection ability. At the same time, the structure and composition depend on the layer forming conditions. To favor the formation of a phase layer with sufficient blocking properties, water hardness and pH should be increased, and in the anionic water composition, carbonate should prevail.

Another typical approach is the installation of previously isolated pipes that already have corrosion-resistant coating on the inner side: zinc or enamel [8]. The most efficient protection is achieved with zinc coating because it protects the pipe metal both mechanically and electrochemically. However, once the coating is damaged, the corrosion process progresses, especially in low conducting water.

Zinc is used because it has low electrochemical potential and will act as anode in contact with steel. Moreover, magnesium and aluminum have similar electrochemical properties [9]. But these metals are not deposited as coatings inside the

pipe. However, magnesium is frequently used as a sacrificial anode for external and internal corrosion protection. Application of electrochemical protection reduces the corrosion rate of protected metals and favors the pH increase due to favorable oxygen reduction on the surface of the protected metal. The application of internal electrochemical protection with sacrificial anode is used in water tanks and reservoirs [10]. Moreover, cathodic protection of internal pipe surfaces is used in highly conductive media [11, 12].

The aim of the present work is to estimate the efficacy and radius of electrochemical protection of the inner pipe surface and protective phase layer formation on the inner side of steel pipes when magnesium is anodically dissolved in hot potable water.

2. Theoretical Calculations

Thermodynamic instability of steel in the presence of oxygen leads to unavoidable corrosion of steel equipment. Steel corrosion in water is an electrochemical process that includes two half-reactions occurring on separate places of the surface.

Anodic reaction of iron ionization:

$$\mathrm{Fe} = \mathrm{Fe}^{2+} + 2e. \tag{1}$$

Cathodic reaction of oxygen reduction:

$$\mathrm{O_2} + 2\mathrm{H_2O} + 4e = 4\mathrm{OH}^-. \tag{2}$$

The corrosion diagram for steel in tap water is given in Figure 1. The anodic part of polarization dependence shows anodic dissolution of iron in low conductive media. The cathodic part of the curve corresponds to oxygen reduction at limiting current $i_{\mathrm{lim}}^{\mathrm{O_2}}$ due to limited oxygen supply to the metallic surface. The rate of oxygen supply determines the corrosion rate of the metal in these conditions.

Cathodic protection is a well-known electrochemical technique used to protect metal equipment from corrosion in conductive environments, such as soil or sea water [13–16]. The protected metal is connected to the negative pole of the current supply source, while the sacrificial anode is connected to the positive one. The idea of cathodic protection is to substitute the electrons of the metal, consumed by the oxygen, with the electrons from the electric network. So, when the metal does not lose electrons, it does not corrode. The protection criterion used in cathodic protection to determine whether the steel is protected is the complete cathodic protection potential E_{ccp}. For steel, this value is $E_{\mathrm{ccp}} = -0.74$ V/SSCE (where SSCE is a saturated silver chloride electrode, $E = 0.2$ V/NHE). According to the diagram (Figure 1), the potential should be shifted from E_{corr} to E_{ccp} and the imposed cathodic current required to shift the steel potential equals 1 A/m^2. To shift the potential, the voltage should be applied between the pipe and the counter electrode. Soluble or inert counter electrodes are both used for cathodic protection, and in the present study, a soluble magnesium electrode was used.

The applied voltage, needed to shift the potential, consists of several terms: potential difference between E_{corr} and E_{ccp}, voltage drop in the metal and in the electrolyte, and

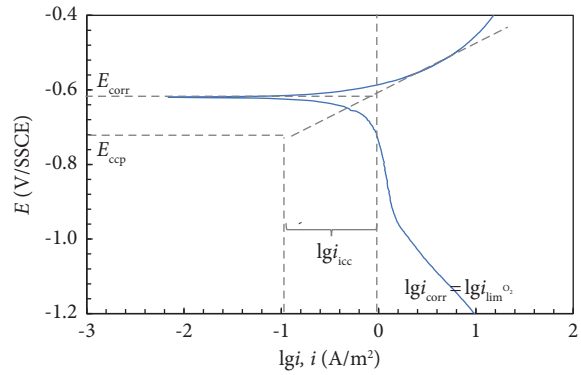

Figure 1: Corrosion diagram of steel in tap water.

polarization drop. In sea water as well as in soil, the conductivity is good enough, so the highest voltage drop is located at the metal/solution interface, but not in the electrolyte. However, when the current is distributed inside the water supply pipe, the cross section is limited, and the conductivity is smaller compared to sea water. In these conditions, the distribution of cathodic protection might be limited by water conductivity [17]. The distribution of cathodic current inside the pipe section was modelled using computer simulation.

The computer model of current distribution inside the pipe was created in COMSOL Multiphysics 5.2. The magnesium anode was located inside the steel pipe, filled with potable water. The conductivity of water in the model corresponds to 250 ppm and equals 450 μS/cm.

Electrochemical processes in the model are as follows:

(i) Anodic dissolution of magnesium from magnesium anode:

$$Mg = Mg^{2+} + 2e, \qquad E = \frac{-1.4\mathrm{V}}{\mathrm{SSCE}}. \tag{3}$$

(ii) Cathodic reduction of oxygen (2) on the surface of steel pipe with the corrosion potential of $E_{\mathrm{corr}} = -(0.62V/\mathrm{SSCE})$.

The applied voltage between the magnesium anode and steel pipe was 1.1 V, and the current was 0.1 A. The distribution of the electric field is shown in Figure 2(a). Figure 2(b) shows the current distribution along the upper pipeline while Figure 2(c) shows that along the lower one. It is clearly seen that the cathodic protection field does not spread far from the anode due to low water conductivity. So, cathodic protection would not be expected to be efficient in distances longer than 15–20 cm from the magnesium anode.

3. Experimental

The tests were performed in a laboratory setup specially designed for the study (Figure 3). The setup consisted of a closed loop (1), made of 50 mm polypropylene (PP) pipes. The volume of the loop was 10 L. The water flow rate was

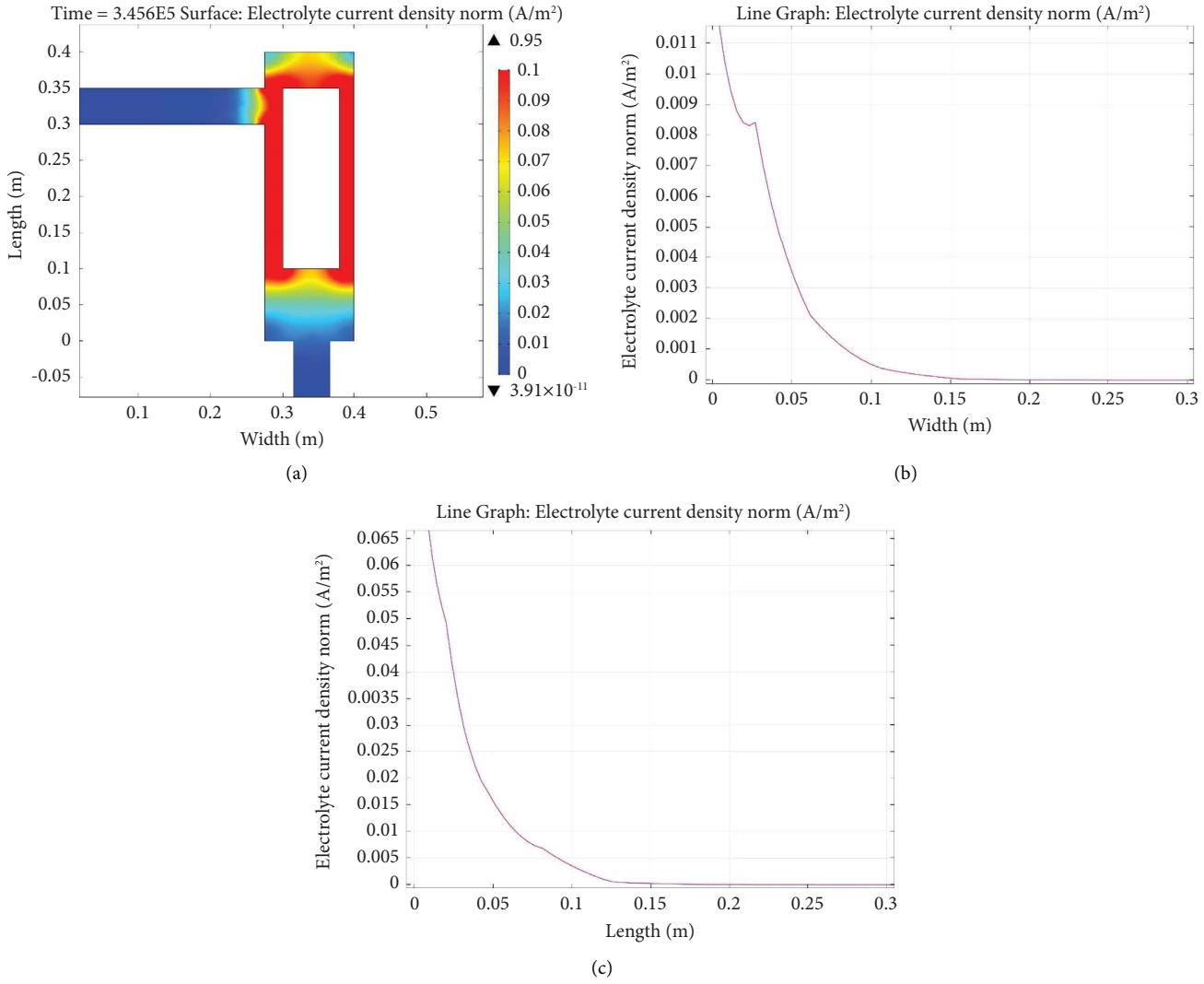

Figure 2: Imposed cathodic current distribution in the electrolyte: (a) around the magnesium anode; (b) along the upper pipeline; (c) along the lower pipeline.

maintained with a centrifugal pump (3), and the water temperature was kept constant during the test with an electric water heater (2).

In the loop, a steel unit (4) was installed, and a magnesium anode (5) was placed inside this unit. The magnesium anode was connected to the positive pole of DC power supply, and the body of the steel unit was connected to the negative one.

Five two-electrode LPR corrosion probes (6) were placed around the loop: one in the largest distance from the anode (2 m away from the anode), two just before and after the steel unit (15–20 cm away from the anode), and the last two in the same distance from the inlet in outlet pipes of the unit (1 m away from the anode). The information about each probe is summarized in Table 1. The negative pole of the DC power supply was also connected to each of the corrosion probes through the switch. The corrosion probes were connected either to the DC power supply for 30 min or to the corrometer for 15 min.

The working electrodes for corrosion studies were manufactured from mild steel St20 (European analog Fe37-3FN or ASTM A48-94a: 1994) in the shape of cylinders of 15 mm length and 6 mm diameter. The area of each electrode was 3 cm^2. The surface of the electrodes was polished before each test with P500 SiC emery paper, degreased, and etched in 200 g/L HCl. The electrodes were weighed to 0.1 mg accuracy before the test for weight loss corrosion rate determination according to the standard ASTM G4-01 (2014). Each pair of electrodes served as a two-electrode linear polarization resistance (LPR) corrosion probe.

Corrosion rate was measured using the electrochemical technique of LPR according to the standard ASTM G96-90 (2018) in galvanostatic mode [18]. The current of 5 $\mu A/cm^2$ density was applied to the probe for 40 sec, and the resulting voltage was measured. The initial potential difference between the electrodes and the solution ohmic drop was compensated, and the corrosion rate was calculated using the conventional B value in Stern–Geary equation of 26 mV.

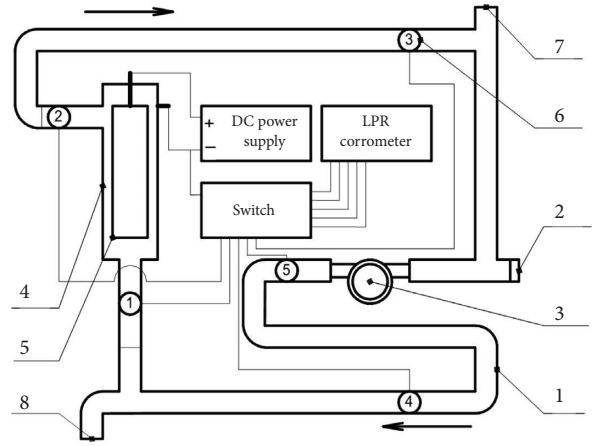

Figure 3: The scheme of laboratory setup: 1—closed water circuit; 2—electric heater; 3—centrifugal pump; 4—steel unit; 5—magnesium anode; 6—LPR corrosion probes (1–5); 7—water inlet; 8—water outlet. Arrows indicate the water flow direction.

Table 1: Corrosion probe's location along the water circuit.

Probe number	Distance from the steel unit along the water flow (m)	Relative distance from the steel unit along the water flow (%)	Distance to magnesium anode (m)
Probe 2	0.2	5	0.2 (outlet of steel unit)
Probe 3	1.0	25	1.0
Probe 5	2.0	50	2.0
Probe 4	3.0	75	1.0
Probe 1	3.8	95	0.2 (inlet of steel unit)

The results of the measurements were recorded and plotted vs. time to examine corrosion rate reduction with time.

Three different tests were performed. The first experiment was blank, where no polarization of magnesium anode or electrodes was applied. In the second experiment, magnesium dissolution was coupled to the cathodic protection of the steel unit. In the third experiment, both the steel unit and all five corrosion probes were connected to the negative pole of DC power supply, while the magnesium anode was connected to the positive one. The applied voltage was 1.1 V, and the resulting current was 0.1 A. The current flowing through each electrode of each corrosion probe was measured daily using UNI-T 65B Digital Multimeter with 0.1 μA accuracy.

Each test continued for 270 hours (two weeks). In the daily hours, the pump and water heater were turned on, the water flow rate was maintained at 0.2 m/s, and temperature was maintained at 45 ± 2 C. The total dissolved solids value in water was 250 ppm. In the night hours and during weekends, the setup was turned off but kept filled with water. A 6 L portion of water was replaced daily by the supply of fresh water. Water parameters were tested during one-day run, namely, pH, calcium, hardness, alkalinity, and total dissolved solids. These data were used to calculate the Langelier saturation index [19].

When the test was ended, the corrosion rate was determined gravimetrically by measuring the weight loss of each electrode of the corrosion probes. Loose corrosion products from the electrode surface were removed mechanically with soft rubber, while dense and adherent rust was chemically dissolved in 5 M H_2SO_4 + 5 g/L thiourea. The electrodes were washed, dried, and weighed to 0.1 mg accuracy, and the corrosion rate was calculated.

The corrosion reduction efficiency was estimated by calculating the degree of protection γ. γ shows the degree of corrosion reduction when corrosion protection is applied and is calculated using the following equation:

$$\gamma = \frac{\mathrm{CR}}{\mathrm{CR}_{\mathrm{prot}}}, \tag{4}$$

where CR is the corrosion rate of steel without any corrosion protection applied (mm/year) and $\mathrm{CR}_{\mathrm{prot}}$ is the steel corrosion rate in conditions of applied corrosion protection (mm/year).

4. Results

The corrosion rate values obtained from weight loss measurements after 2 weeks of electrode exposure in the laboratory setup are given in Figure 4(a), and the calculated degree of protection is given in Figure 4(b).

Corrosion rates obtained from LPR measurements are presented in Figure 5. Corrosion rate variation vs. time provides information about the blocking properties of the

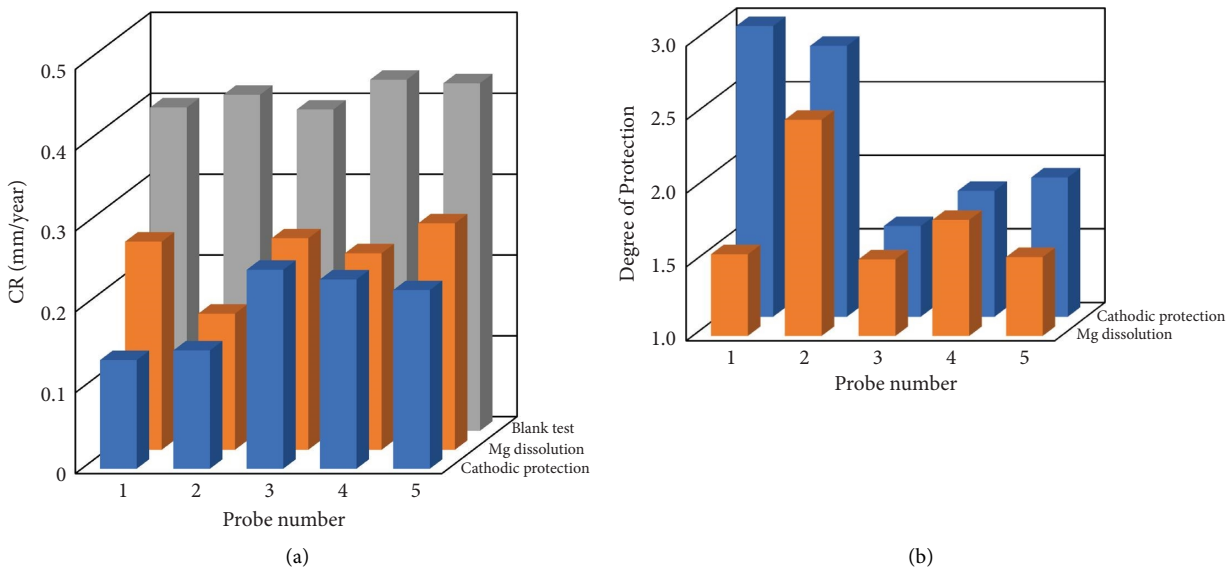

Figure 4: Weight loss corrosion rate and degree of protection with magnesium anode dissolution in tap water depending on the test conditions.

surface layer because the cathodic polarization was turned off during LPR measurements.

Water parameters were measured after each test, and the results are presented in Table 2. These parameters were used to calculate the Langelier saturation index.

Cathodic current passing through each corrosion probe was measured daily for the 2-week test. The results are given in Figure 6. Noticeable cathodic current was measured only with probes 1 and 2 placed in the shortest distance from the anode (15 cm). The cathodic current on probes 3–5, placed in the distance 1-2 m from the magnesium anode, was hard to register due to low water conductivity. Current-time dependence shows a decreasing trend and finally halves in the end of two weeks.

5. Discussion

Steel corrosion rate in tap water without any protection in the two weeks was relatively high, around 0.4 mm/year (Figure 4(a)). The data obtained with LPR technique appeared to be higher (0.5–0.7 mm/year) because weight loss measurements included night hours and weekends, while LPR was only measured during 8 hours per day. According to corrosion time dependence (Figure 5(a)), the corrosion rate shows a decreasing tendency. For probes 1, 2, and 4, the corrosion rate reached a constant level in 2-3 days, while that for probes 3 and 5 slowly decreased for two weeks.

Corrosion reduction is a result of surface layer formation from corrosion products and hardness salts. The LPR technique provides a possibility to estimate the protective properties of the surface layers. Low corrosion rate means that on the electrode surface, a barrier layer is formed, preventing oxygen supply to the surface.

The formation of carbonate deposits has the following mechanism. Oxygen reduction by reaction (2) leads to the formation of OH^- that shifts calco-carbonic equilibrium in the preelectrode layer:

$$HCO_3^{2-} + OH^- = CO_3^{2-} + H_2O. \quad (5)$$

In the presence of Ca^{2+} ions, calcium carbonate precipitates, forming a phase layer at the interface, thus reducing the oxygen supply to the surface:

$$Ca^{2+} + CO_3^{2-} = CaCO_3. \quad (6)$$

The ability to form or dissolve calcium carbonate determines the corrosion aggressivity of the water and can be estimated with the Langelier saturation index. Positive index value suggests that water can form calcium deposits, and such water is believed to be nonaggressive, while negative index values mean the water can dissolve carbonate deposits on the metal surface and can cause corrosion speed-up.

Calculated indices for fresh water and after the blank test are presented in Table 1. The Langelier index for tap water is 1.3, so the water is nonaggressive. After the two-week test, the index shows a slight increase (LI = 1.4), due to pH increase.

When magnesium is anodically dissolved, the corrosion rate of all probes is reduced in 1.5-2.3 times compared to their corrosion rate in blank experiment (Figure 5(b)). According to LPR data, the corrosion rate decreases in the first 3 days, reaching a stable value, and does not change significantly for the rest of time. Calculated oxygen consumption during electrolysis shows that its concentration is reduced only by 10%. However, the obtained Mg^{2+} and OH^- ions increase total alkalinity and pH, so LI increases to 2.3 after the test with magnesium anode dissolution, meaning that the water becomes less aggressive. The achieved corrosion rate appeared to be dependent on the location of the corrosion probe. The most efficient corrosion reduction is

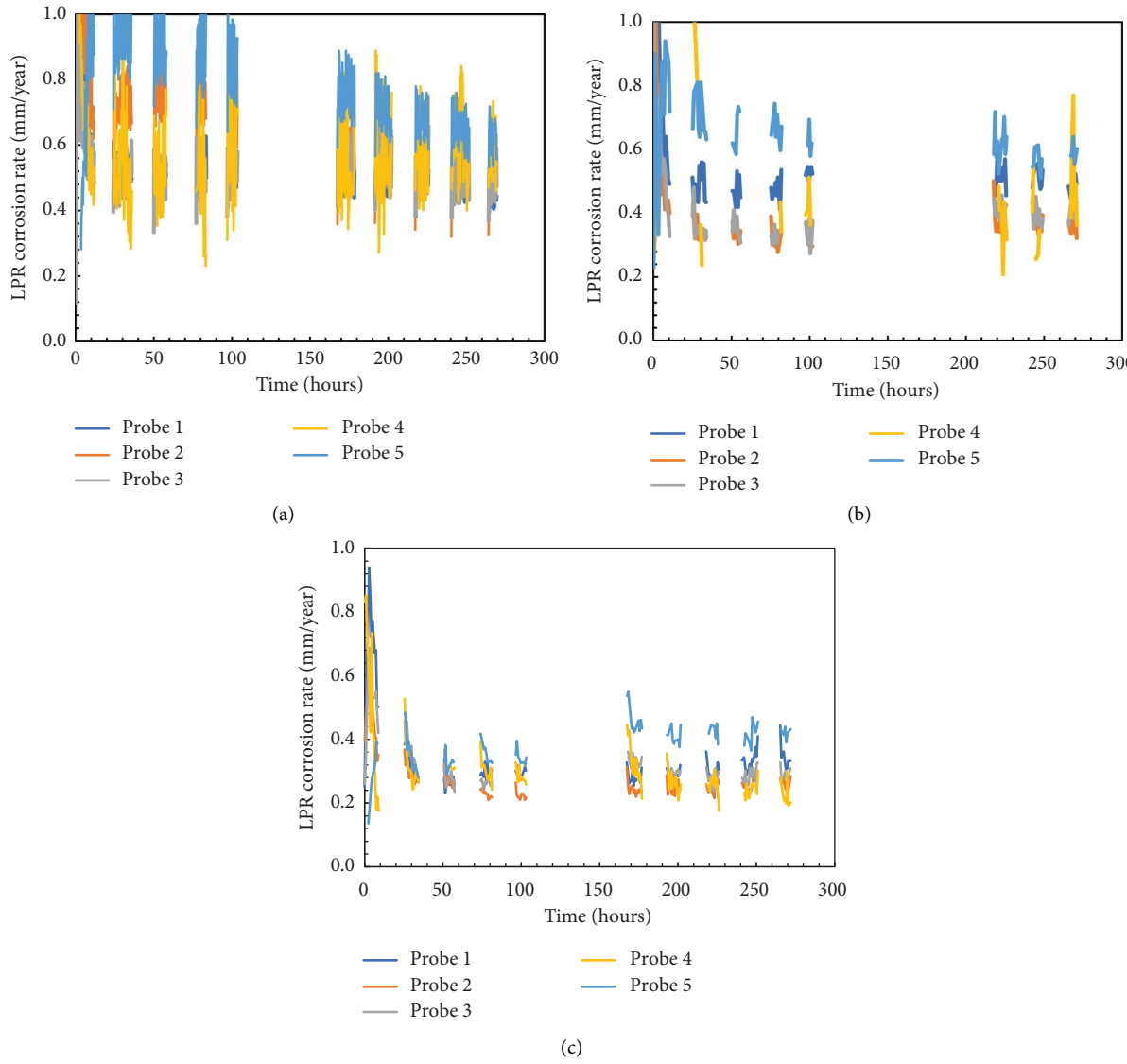

Figure 5: Time dependence of LPR corrosion rate in tap water depending on the test conditions: (a) the electrodes corrode in natural conditions; (b) the magnesium dissolution takes place in the setup (0.1 A applied current); (c) the magnesium dissolution takes place in the setup (0.1 A applied current) and the probe's electrodes are connected as cathodes (cathodic protection).

Table 2: Water parameters in tap water depending on the test conditions.

No.	Conditions	TDS (mg/L)	Calcium hardness (mg/L)	Total alkalinity (mg/L)	Water temperature (°C)	pH	pH_s	LI
1	Fresh water	220	200	100	45	8.20	6.9	1.3
2	Blank experiment	160	100	50	45	8.90	7.5	1.4
3	Magnesium dissolution	290	100	200	45	9.20	6.9	2.3

obtained with probe 2 located just in the outlet of the steel unit where magnesium dissolution occurs. Newly formed Mg^{2+} and OH^- ions move with the water flow and cover the surface of the corrosion probe with a dense layer, reducing the corrosion rate.

The results of cathodic polarization of corrosion probes are consistent with the computer modelling (Figure 2). The cathodic current is registered only with probes 1 and 2, located near the magnesium anode (Figure 3). Measured cathodic current density was 1 A/m^2, which is enough to reach complete cathodic protection of the steel according to the corrosion diagram (Figure 1). However, electrodes 3–5 are not influenced by the cathodic protection because of low water conductivity. The electric field simply does not reach these probes and they remain unprotected. So, the corrosion rate of probes 3–5 reaches the same values as in the test without cathodic protection.

Application of cathodic protection to probes 1 and 2, installed close to the magnesium anode, coupled with the increased Langelier index, favors the formation of the

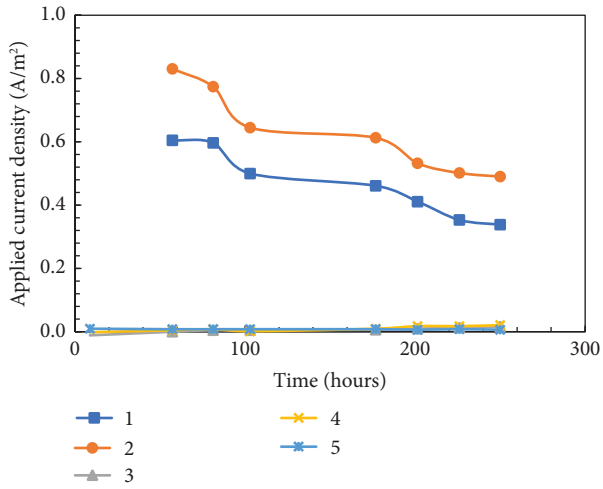

Figure 6: The cathodic current density depending on the probe number.

protective carbonate layer on the surface of probes. The degree of protection of probes 1 and 2 is nearly the same, 2.98 and 2.84 times. Combination of cathodic protection with reduction of water aggressivity provides the formation of a carbonate layer on the whole surface of the metal, while when no cathodic protection is applied, the carbonate layer is formed only on the regions of the surface where oxygen is reduced. Thus, some regions of the surface will remain uncovered with calcium carbonate. However, the cathodically unprotected regions of the pipe are still protected with a phase layer of calcium carbonate, formed as a sequence of increased Langelier index. So, even in low conducting media, the dissolution of magnesium anode provides distinguishable corrosion protection of the steel pipe. The negative impact of long-term exposure of metal pipe in water that produces scale is that the inner section of pipe reduces and can lead to the increase of a pressure drop over the narrow sections.

The results obtained in the present study provide the information of the action radius of combined action of cathodic protection and magnesium dissolution. In low conductivity water, protected distance, where both cathodic protection and magnesium dissolution are involved, spreads only in 10–15 cm around the magnesium anodes. In the case of the closed loop, all remaining surfaces will be protected by the formation of calcium carbonate layer at a free corrosion potential of the steel, and the degree of protection without cathodic protection reaches 1.5–1.9 times.

6. Conclusions

The distribution of cathodic protection inside the water pipes was investigated using the computer model and experimental testing. Both techniques showed that for low conductive media (TDS = 250 ppm), the protection field spreads only 15 cm around the anode. The part of the pipe located outside this region is unprotected because the electric field has no effect over it.

The dissolution of magnesium anode leads to the increase of water pH value and alkalinity. Thus, the water saturation index increases and the steel corrosion rate decreases in 1.5 times. The calcium carbonate deposits on the steel surface forming a protective layer. Long exposure of pipe in scale forming conditions may cause cross section reduction and possible pressure losses.

On the cathodically protected steel surface, the calcium carbonate layer with better protection properties is formed. The degree of protection on the cathodically protected steel surface reaches 2.9 times. The obtained results can be further utilized to improve the performance of hot water supply systems.

Data Availability

All data generated or analyzed during this study are included within the article.

Conflicts of Interest

The authors declare that they have no conflicts of interest.

References

[1] V. S. Marangou and K. Savvides, "First desalination plant in Cyprus-product water aggresivity and corrosion control," *Desalination*, vol. 138, no. 1-3, pp. 251–258, 2001.

[2] H. M. Müller-Steinhagen and C. A. Branch, "Comparison of indices for the scaling and corrosion tendency of water," *Canadian Journal of Chemical Engineering*, vol. 66, no. 6, pp. 1005–1007, 1988.

[3] T. Y. Mankikar, "Comparison of indices for scaling and corrosion tendency of groundwater: case study of unconfined aquifer from Mahoba District, U.P. State," *Applied Water Science*, vol. 11, no. 6, p. 94, 2021.

[4] G. S. Vasyliev, Y. S. Gerasimenko, S. K. Poznyak, and L. S. Tsybulskaya, "A study of the anticorrosion properties of carbonate deposits to protect low-carbon steel from the action of tap water," *Russian Journal of Applied Chemistry*, vol. 87, no. 4, pp. 450–455, 2014.

[5] G. S. Vasyliev, "The influence of flow rate on corrosion of mild steel in hot tap water," *Corrosion Science*, vol. 98, pp. 33–39, 2015.

[6] G. S. Vasyliev, "Adaptation of the method of polarization resistance to the evaluation of corrosion rate in the formation of deposit of difficultly dissolved iron oxides," *Materials Science*, vol. 55, no. 1, pp. 130–135, 2019.

[7] N. Atanov, P. Gorshkalev, M. Chernosvitov, and A. Smirnova, "Pipelines corrosion during water supply process," *IOP Conference Series: Materials Science and Engineering*, vol. 365, Article ID 42073, 2018.

[8] M. Zhang, H. Wang, T. Nie, J. Bai, F. Zhao, and S. Ma, "Enhancement of barrier and anti-corrosive performance of zinc-rich epoxy coatings using nano-silica/graphene oxide hybrid," *Corrosion Reviews*, vol. 38, no. 6, pp. 497–513, 2020.

[9] I. Gurrappa, "Cathodic protection of cooling water systems and selection of appropriate materials," *Journal of Materials Processing Technology*, vol. 166, no. 2, pp. 256–267, 2005.

[10] J. Kou, X. Zhang, G. Cui, and X. Yin, "Research progress on the cathodic protection current and potential distribution of the tank bottom plate," *Corrosion Reviews*, vol. 34, no. 5-6, pp. 277–293, 2016.

[11] J. A. Jeong, M. Kim, and D. H. Lee, "Electrochemical and on-site tests for the application of cathodic protection on the inner surface of seawater pipes," *Journal of the Korean Society of Marine Engineering*, vol. 43, no. 8, pp. 610–617, 2019.

[12] K. McChesney, M. Trask, D. Penner et al., "Internal cathodic protection to study the erosion-corrosion of AISI 1018 carbon steel," *Canadian Journal of Chemical Engineering*, vol. 100, pp. 35–43, 2021.

[13] J. George, "Corrosion Study on Protected and Unprotected Underground Pipe by Manipulating Soil Conditions," *NACE - International Corrosion Conference Series*, Onepetro, Richardson, TX, USA, 2018.

[14] D. Lauria, S. Minucci, F. Mottola, M. Pagano, and C. Petrarca, "Active cathodic protection for HV power cables in undersea application," *Electric Power Systems Research*, vol. 163, pp. 590–598, 2018.

[15] M. S. Hong, Y. S. So, and J. G. Kim, "Optimization of cathodic protection design for pre-insulated pipeline in district heating system using computational simulation," *Materials*, vol. 12, no. 11, p. 1761, 2019.

[16] A. Goyal, E. K. Olorunnipa, H. S. Pouya, E. Ganjian, and A. O. Olubanwo, "Potential and current distribution across different layers of reinforcement in reinforced concrete cathodic protection system-a numerical study," *Construction and Building Materials*, vol. 262, p. 120580, 2020.

[17] X. N. Z. C. Z. F. Cuihong, "Potential distribution on cathodically protected internal surface of pipe," *Journal of Chinese Society for Corrosion and Protection*, vol. 7, pp. 249–256, 1987.

[18] H. S. Vasyl'ev and Y. S. Herasymenko, "Corrosion meters of new generation based on the improved method of polarization resistance," *Materials Science*, vol. 52, no. 5, pp. 722–731, 2017.

[19] K. Rafferty, *Scaling in Geothermal Heat Pump Systems. Report*, Geo-Heat Center Oregon Institute of Technology, Klamath Falls, OR, USA, 2000.